DOI: 10.1002/ejoc.200800045

Heterocyclic Quinol-Type Fluorophores: Solid-State Fluorescence Change in Crystals of Benzo[*b*]naphtho[1,2-*d*]furan-6-one-Type Fluorophore upon Inclusion of Organic Solvent Molecules[‡]

Yousuke Ooyama*[a] and Katsuhira Yoshida*[a]

Keywords: Fluorescence / Dyes / Inclusion compounds / Crystal structures / Oxygen heterocycles

The crystals of benzo[*b*]naphtho[1,2-*d*]furan-6-one-type fluorophores (**1**) exhibit sensitive colour and fluorescence change upon enclathration of organic solvent molecules. The crystal of fluorophore **1b** (R = Bu) exhibits fluorescence decrease upon inclusion of cyclohexane; however, the crystal of fluorophore **1c** (R = Ph) exhibits a drastic fluorescence enhancement upon inclusion of chloroform. To elucidate the enclathrated guest effects on the photophysical properties of the crystals, the X-ray crystal structures of the guest-free and guest-inclusion compounds were determined. On the basis of the spectroscopic data and the crystal structures, the effects of the enclathrated guest on the solid-state photophysical properties of the clathrate compounds are discussed.

Introduction

The development of fluorescent molecular sensors is of importance because they can be used in the detection of cations and anions and in biochemical analyses, for example, in the detection of amino acids; they can also be used as fluorescent switches.[1] A number of fluorophores have been developed, and the relation between the chemical structure and their fluorescence properties in solution have been investigated in order to elucidate the mechanism of fluorescence changes upon formation of complexes with cations, anions and neutral molecules.[2] However, only several fluorescent hosts that exhibit fluorescence change upon enclathration of organic solvent molecules in the crystalline state have been reported.[3]

We recently developed benzofurano[3,2-*b*]naphthoquinol-type,[4] imidazo[5,4-*a*]anthraquinol-type[5] and phenanthro[9,10-*d*]imidazole-type[6] fluorescent hosts whose crystals exhibit a dramatic fluorescence enhancement upon inclusion of various gaseous amines, organic solvents and carboxylic acids, respectively. From the relation between the solid-state fluorescence properties and the crystal structures, it was confirmed that the destruction of π–π interactions between the fluorophores by guest enclathration is the main reason for the guest-dependent fluorescence enhancement behaviour. In a previous paper, we reported the absorption and fluorescence properties in solution and in the solid state of heterocyclic quinol-type fluorophores, 5-hydroxy-5-substituted benzo[*b*]naphtho[1,2-*d*]furan-6-one (**1**) and 3-hydroxy-3-substituted benzo[*kl*]xanthen-2-one (**2**) fluorophores (Scheme 1).[7] Here, we report sensitive colour and fluorescence changes in quinol **1** upon enclathration of organic solvent molecules in the solid state. The X-ray crystal structures of **1** and its guest-inclusion compounds have been determined, on the basis of which the enclathrated guest effects on the solid-state fluorescence properties are discussed.

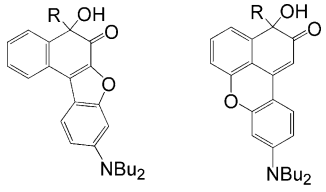

1a: R=Me
1b: R=Bu
1c: R=Ph

2a: R=Me
2b: R=Bu
2c: R=Ph

Scheme 1. Heterocyclic quinol-type fluorophores **1a**–**c** and **2a**–**c**.

Results and Discussion

Inclusion Ability in the Crystalline State

In order to investigate their inclusion ability, we recrystallized the quinol compounds from various organic solvents such as ethanol, acetonitrile, cyclohexane, chloroform, benzene, 1,4-dioxane and morpholine. Quinols **1a**

[‡] Heterocyclic Quinol-Type Fluorophores, 7. Part 6: Y. Ooyama, T. Mamura, K. Yoshida, *Eur. J. Org. Chem.* **2007**, 30, 5010–5019.

[a] Department of Material Science, Faculty of Science, Kochi University
Akebono-cho, Kochi 780-8520, Japan
Fax: + 81-88-844-8359
E-mail: kyoshida@cc.kochi-u.ac.jp
yooyama@hiroshima-u.ac.jp

and **2a**–**c** did not form any inclusion compounds. However, we found that quinols **1b** and **1c** yield inclusion compounds in stoichiometric ratios with cyclohexane and chloroform, respectively. Relative to the inclusion ability of the 1,4-quinol-type fluorescent hosts benzofurano[3,2-*b*]naphthoquinol-type[4] and imidazo[5,4-*a*]anthraquinol-type[5] fluorophores, that of the 1,2-quinol-type fluorescent hosts benzo[*b*]naphtho[1,2-*d*]furan-6-one (**1**) and benzo[*kl*]xanthen-2-one (**2**) fluorophores was extremely poor. Crystals of **1b**·cyclohexane (host/guest, 2:1) were recrystallized from cyclohexane as greenish-yellow prisms. In contrast, the crystals of **1c**·chloroform (host/guest, 1:1) were recrystallized from chloroform as greenish-yellow prisms. Furthermore, a drastic fluorescence change upon inclusion of guest molecules was observed in both the crystals of **1b**·cyclohexane and **1c**·chloroform.

Solid-State Fluorescence Change upon Formation of Guest-Inclusion Crystals

In order to investigate the effect of clathrate formation on the solid-state photophysical properties, the fluorescence excitation and emission spectra of the guest-free and the guest-inclusion crystals were measured (Figures 1 and 2). Relative to the guest-free crystals of **1b**, the excitation and emission maxima of the crystals of **1b**·cyclohexane are little affected: the guest-free host crystal exhibits relatively strong fluorescence with emission maximum at 530 nm, whereas the crystals of **1b**·cyclohexane exhibit weak fluorescence intensity with the emission maximum at 527 nm, whose intensity is reduced to ca. 35%. In contrast, the excitation and emission maxima of the crystals of **1c**·chloroform exhibit a blueshift and the fluorescence intensity is greatly enhanced in comparison with that of the guest-free crystal of **1c**: the fluorescence intensity of **1c**·chloroform was ca. threefold higher.

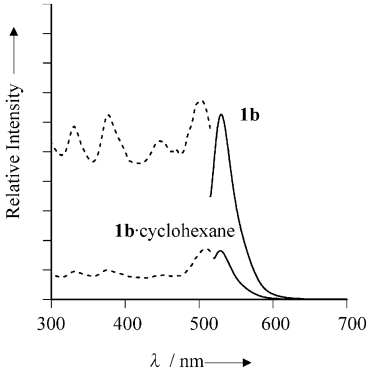

Figure 1. Excitation (- - -) and emission (—) spectra of the crystals of **1b** and **1b**·cyclohexane: **1b**: λ_{ex} = 503 nm, λ_{em} = 530 nm; **1b**·cyclohexane: λ_{ex} = 505 nm, λ_{em} = 527 nm.

Interestingly, when the guest-free crystals of **1c** were placed in a vessel saturated with chloroform vapour at 30 °C, the colour of the crystals turned from yellow to greenish-yellow. The changes in the solid-state fluorescent excitation and emission spectra of **1c** upon exposure to chloroform vapour were investigated (Figure 3). We found that a hypsochromic shift in the excitation and emission maxima and a drastic fluorescence enhancement are induced upon formation of an inclusion compound with chloroform. The initial excitation band at 519 nm shifted to 507 nm. The corresponding fluorescence spectra showed an increase in fluorescence intensity with a blueshift in the emission maximum from 558 to 530 nm. The formation of clathrate (**1c**/chloroform, 1:1) was suggested from integration of the signals in the ^{1}H NMR spectrum. The host/guest ratio is 1:0.5 when the crystals were exposed to chloroform vapour for 30–40 min. It took about 150 min to reach the final saturated excitation and emission spectra, which were in good agreement with the spectra of the clathrate compound (**1c**/chloroform, 1:1) obtained by recrystallization of compound **1c** from chloroform.

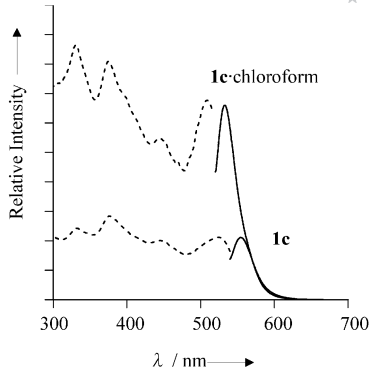

Figure 2. Excitation (- - -) and emission (—) spectra of the crystals of **1c** and **1c**·chloroform: **1c**: λ_{ex} = 519 nm, λ_{em} = 558 nm; **1c**·chloroform: λ_{ex} = 509 nm, λ_{em} = 533 nm.

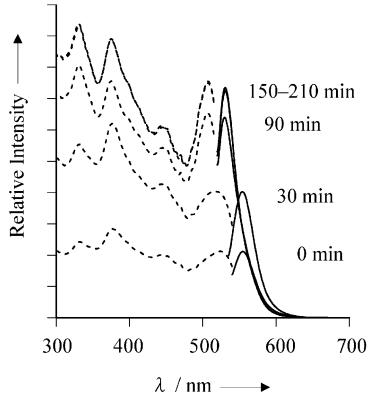

Figure 3. Time-dependent spectral changes in the guest-free crystals of **1c** upon exposure to chloroform vapour at 30 °C; the excitation (- - -) and emission (—) spectra were recorded at their corresponding emission and excitation maxima.

Relation between the Solid-State Fluorescence Properties and X-ray Crystal Structures of the Guest-Free and Guest-Inclusion Compounds

In order to investigate the enclathrated guest effects on the fluorescence properties of the crystal, the crystal struc-

tures of the guest-free and the guest-inclusion compounds were determined by X-ray diffraction analysis (Figures 4, 5 and 6). The packing structures demonstrate that the quinol molecules of **1a**, **1b**, **1c** and **1b**·cyclohexane are arranged in a "tread on staircase" fashion. In contrast, the packing structure of **1c**·chloroform demonstrates that the quinol molecules are arranged in a "bricks in a wall" fashion. All crystal structures are built up by a centrosymmetric dimer unit that is composed of a pair of quinol enantiomers. In the crystals of **1a**, **1b**·cyclohexane, **1c** and **1c**·chloroform, neighbouring enantiomers are connected by two intermolecular hydrogen bonds between the hydroxy and carbonyl oxygen atoms through the hydroxy proton: O(1)···O(2)* distances for **1a**, **1b**·cyclohexane, **1c** and **1c**·chloroform are 2.844(3), 2.783(3), 2.812(4) and 2.880(4) Å, respectively. On the contrary, in the crystal of **1b**, there are two crystallographically independent molecules: intermolecular hydrogen bonding is also observed between the hydroxy and carbonyl oxygen atoms through the hydroxy proton of each crystallographically independent molecule [O(1)···O(5) and O(2)···O(4) distances 2.81(1) and 2.77(4) Å, respectively]. Furthermore, the hydroxy proton has two proton acceptors and it becomes bifurcated-donor hydrogen to form the three-centred hydrogen bonding with the above inter- and intramolecular carbonyl oxygen atoms. With respect to intramolecular hydrogen bonding, O(1)···O(2) distances for

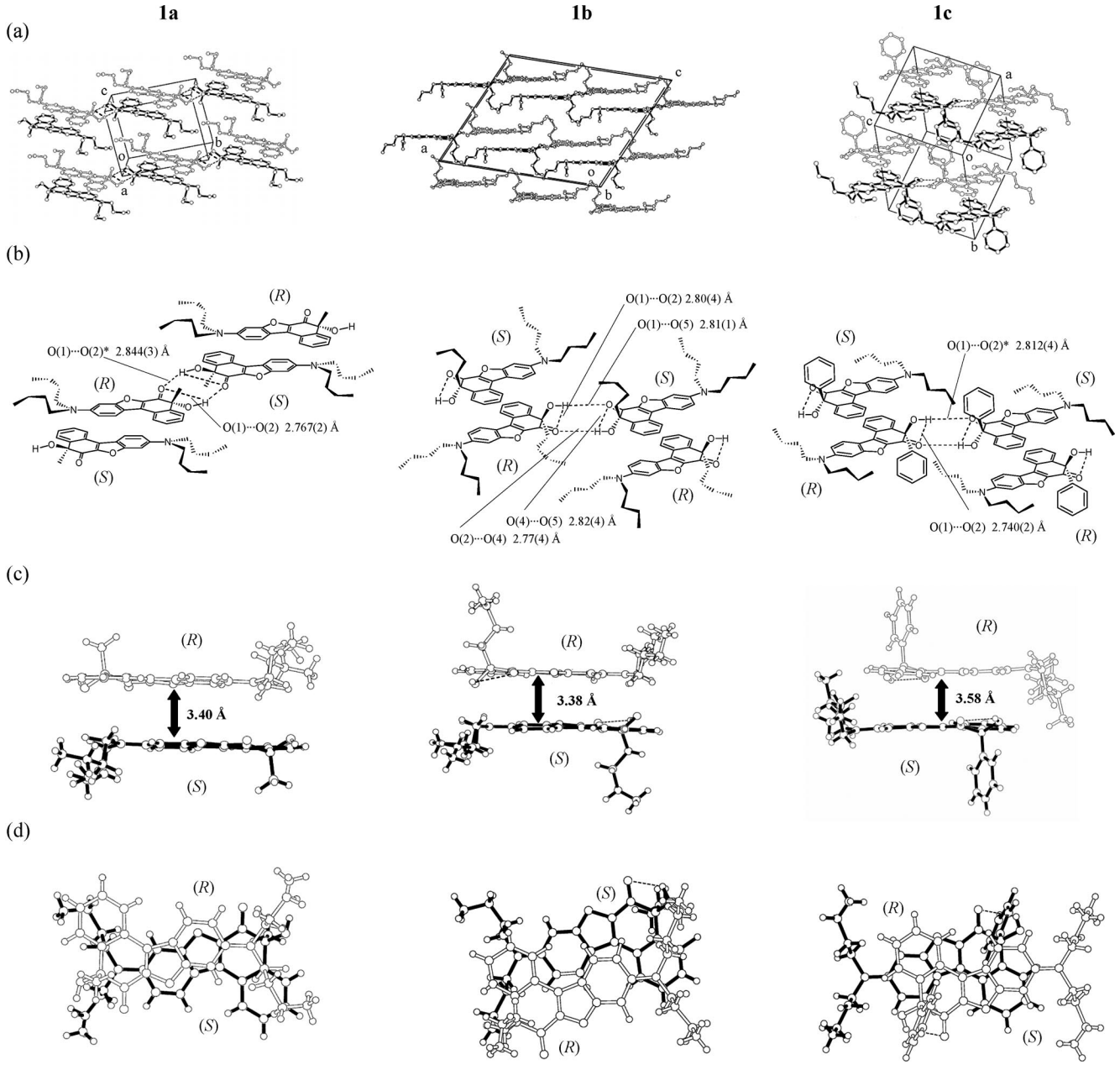

Figure 4. Crystal packing and hydrogen bonding pattern of **1a**–**1c**: (a) a stereoview of the molecular packing structure, (b) a schematic structure, (c) a side view and (d) a top view of the pairs of fluorophores.

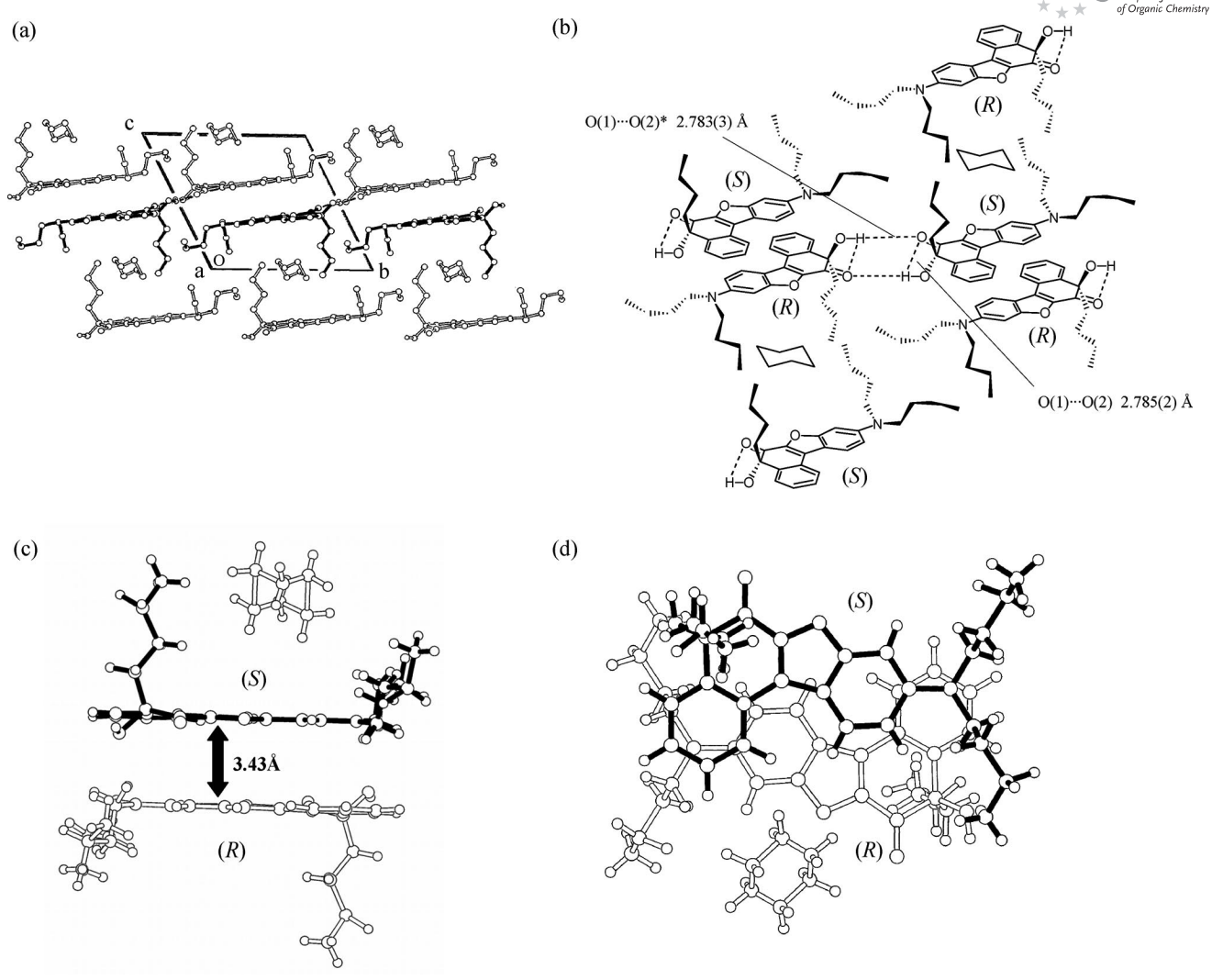

Figure 5. Crystal packing and hydrogen bonding pattern of **1b**·cyclohexane (2:1): (a) a stereoview of the molecular packing structure, (b) a schematic structure, (c) a side view and (d) a top view of a cluster unit.

1a, **1b**, **1c**, **1b**·cyclohexane and **1c**·chloroform are 2.767(2), 2.80(4), 2.740(2), 2.785(2) and 2.738(5) Å, respectively, and the O(4)···O(5) distance for **1b** is 2.82(4) Å.

One feature was particularly interesting in the crystal of **1c**·chloroform (Figure 6c): the chloroform molecules were incorporated among two pairs of quinol enantiomers, and two types of CH···O interactions were formed between the carbonyl group of the host and the proton of chloroform and between the furan oxygen atoms of the host and the proton of chloroform [C(31)···O(2) distance 3.412(7) Å, C(31)···O(3) distance 3.489(8) Å]. In contrast, in the crystal of **1b**·cyclohexane (Figure 5c), the cyclohexane molecules were incorporated in the cavity constituted of a butyl group, and the 9-dibutylamino group is placed on the same side as the π plane, which already exists in the crystal of **1b** (Figure 4c).

Big differences in the π stacking between a pair of quinol enantiomers among the three quinols were observed. In the crystal of **1a**, a pair of quinol enantiomers overlaps the whole molecule from the electron-donor part of the benzofurano moiety containing the 9-dibutylamino group to the electron-acceptor part of the naphthoquinol moiety, which is deeply related to the solid-state photophysical properties. A large redshift in the absorption and fluorescence maxima and the solid-state fluorescence quenching by strong donor–acceptor-type π–π interactions of fluorescent dyes are known.[4–10] In fact, the fluorescence emission intensities of **1a**–**c** are in the order **1c** > **1b** > **1a** in the crystalline state. In the crystal of **1b**, a donor–acceptor-type of π stacking between a pair of quinol enantiomers is observed; however, the range of π stacking is less than that of **1a**. The interplanar distances between the benzofuranonaphthoquinol planes are ca. 3.40, 3.38 and 3.58 Å for **1a**, **1b** and **1c**, respectively. There are seven, four and five short interatomic π–π contacts of less than 3.6 Å in a pair of enantiomers for **1a**, **1b** and **1c**, respectively.

In contrast, in the crystals of **1b**·cyclohexane as shown in Figure 5c,d, a donor–acceptor-type of π stacking between a pair of quinol enantiomers is also formed, and the interplanar distance between the benzofuranonaphthoquinol plates is ca. 3.43 Å. There are 12 short interatomic contacts of less than 3.6 Å, which suggests that stronger π–π interac-

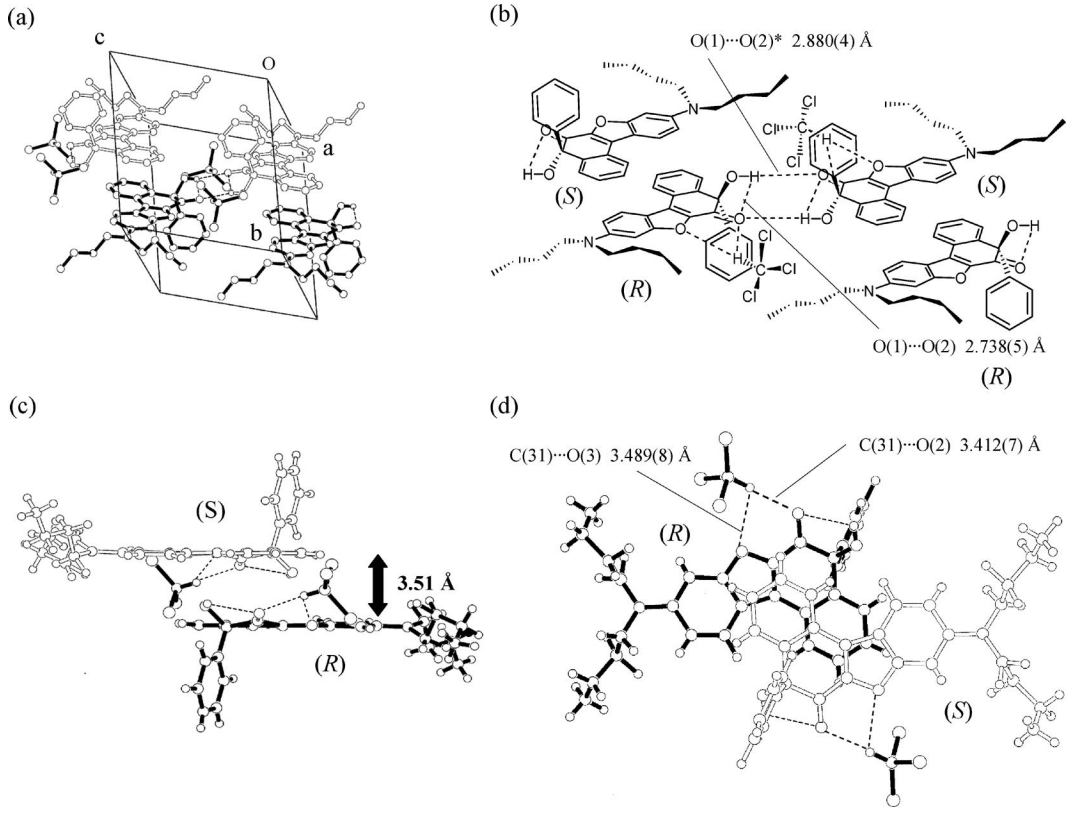

Figure 6. Crystal packing and hydrogen bonding pattern of **1c**·chloroform (1:1): (a) a stereoview of the molecular packing structure, (b) a schematic structure, (c) a side view and (d) a top view of a cluster unit.

tions exist in the cyclohexane-inclusion crystal than in the guest-free crystal of **1b**. In contrast, such a π stacking is not observed for **1c**·chloroform; the enclathrated chloroform disturbs the overlapping of the host aromatic planes. It was confirmed that the enclathrated chloroform molecules considerably weaken the host–host π–π interactions. Therefore, the solid-state fluorescence quenching in the crystal of **1b** are considered to be induced upon inclusion of cyclohexane molecules by the formation of donor–acceptor-type π–π interactions. In the crystals of **1c**·chloroform, it is proved that the destruction of the π–π interactions between the fluorophores by the enclathrated chloroform molecules are the main reason for the fluorescence enhancement and the blueshift in the absorption and fluorescence maxima of the crystals.

By comparing the crystal structures of 1,2-quinols **1a**–**c** with those of the 1,4-quinol benzofurano[3,2-*b*]naphthoquinol-type[4] and imidazo[5,4-*a*]anthraquinol-type[5] fluorophores, we noticed the effects of geometric arrangement on the guest inclusion in the solid state (Figure 7). In the crystals of the 1,4-quinols, the packing structures demonstrate that the crystals are built from a centrosymmetric dimer unit that is composed of a pair of quinol enantiomers bound cofacially by intermolecular hydrogen bonds be-

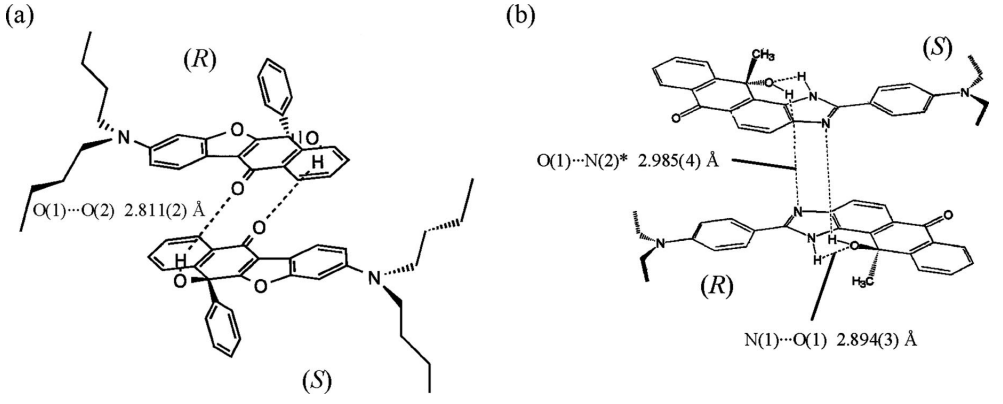

Figure 7. Schematic structure of a pair of quinol enantiomers for (a) benzofurano[3,2-*b*]naphthoquinol-type[4] and (b) imidazo[5,4-*a*]-anthraquinol-type[5] fluorophores. Hydrogen bonds are shown as dotted lines.

tween the hydroxy group and the carbonyl oxygen atom or the imidazole nitrogen atom on both sides of the dimer unit through the hydroxy proton. Conversely, the crystals of 1,2-quinols **1a**–**c** are built from a centrosymmetric dimer unit that is composed of a pair of quinol enantiomers, and neighbouring enantiomers that exist on this plane are connected by two strong intermolecular hydrogen bonds between the hydroxy group and carbonyl oxygen atoms through the hydroxy proton. These results show that the strong intra- and intermolecular hydrogen bonds between the fluorophores such as that observed in the crystals of **1a**–**c** make it difficult to enclathrate the guest molecules in the solid state. Consequently, it is difficult to construct a flexible cavity upon enclathration of organic solvent molecules in the crystals of **1a**–**c**. The inclusion ability of **1a** was extremely poor relative to that of **1b** and **1c**. It was considered that the difficulty of constructing the cavity among the host molecules was a result of small substituents (methyl group) and the formation of strong donor–acceptor-type π–π interactions between the fluorophores in the crystal of **1a**; thus, it was very difficult to enclathrate the guest molecules.

Conclusions

We showed that the crystals of benzo[*b*]naphtho[1,2-*d*]-furan-6-one-type fluorophore (**1**) exhibit sensitive colour and fluorescence change upon enclathration of organic solvent molecules. From comparison of the X-ray crystal structures of the guest-free and its guest inclusion compounds, it was concluded that the decrease or increase in the π–π interactions between the fluorophores by the enclathrated guest molecules are the main reason for changes in the fluorescence properties of the crystals. These results also show that the quinol-type fluorescent hosts can be utilized as a selective chemical sensor for recognition of gaseous organic solvent molecules.

Experimental Section

General: Elemental analyses were measured with a Perkin–Elmer 2400 II CHN analyzer. Single-crystal X-ray diffraction was performed with a Rigaku AFC7S diffractometer. Fluorescence emission and excitation spectra were measured with a JASCO FP-777 spectrometer. For the measurement of the solid-state fluorescence excitation and emission spectra of the crystals, a Jasco FP-1060 attachment was used. ^{1}H NMR spectra were recorded with a JNM-LA-400 (400 MHz) FT NMR spectrometer with tetramethylsilane (TMS) as an internal standard.

Preparation of Guest -Inclusion Crystals of 1b and 1c: Host compound **1b** or **1c** was dissolved with heating in respective guest solvent. The solution was filtered and kept for a few days at room temperature. The crystals that formed were collected by filtration. The host/guest stoichiometric ratio of the inclusion compounds was determined by integration of the signals in the ^{1}H NMR spectra and CHN analysis.

Measurement of the Time-Dependent Spectral Changes of 1c upon Exposure to Chloroform Vapour: The guest-free crystal of host quinol **1c** was placed in a vessel saturated with chloroform vapour at 30 °C. The exposed sample was taken out at different time intervals, and the measurement of the absorption and fluorescence spectra was carried out. The host/guest stoichiometric ratio of the inclusion compound was determined by integration of the signals in the ^{1}H NMR spectrum.

X-ray Crystallographic Studies: The reflection data were collected at 23 ± 1 °C with a Rigaku AFC7S four-circle diffractometer by 2θ–ω scan technique and by using graphite-monochromated Mo-K_α (λ = 0.71069 Å) radiation at 50 kV and 30 mA. In all cases, the data were corrected for Lorentz and polarization effects. A correction for secondary extinction was applied. The reflection intensities were monitored by three standard reflections for every 150 reflections. An empirical absorption correction based on azimuthal scans of several reflections was applied. All calculations were performed by using the teXsan[11] crystallographic software package of Molecular Structure Corporation. CCDC-294660 (for **1a**), -294661 (for **1b**), -294662 (for **1c**), -635414 (for **1b**·cyclohexane) and -635415 (**1c**·chloroform) contain the supplementary crystallographic data for this paper. These data can be obtained free of charge from The Cambridge Crystallographic Data Centre via www.ccdc.cam.au.uk/data_request/cif.

Inclusion Compound 1b·Cyclohexane: Crystals of **1b**·cyclohexane were recrystallized from cyclohexane as air-stable, greenish-yellow prisms. The one selected had approximate dimensions of 0.87 × 0.40 × 0.20 mm. The transmission factors ranged from 0.98 to 1.00. The crystal structure was solved by direct methods by using SIR 92.[12] The structures were expanded by using Fourier techniques.[13] The non-hydrogen atoms were refined anisotropically. Some hydrogen atoms were refined isotropically, the rest were fixed geometrically and not refined. Crystal data: $C_{31}H_{41}NO_3$, M = 475.67, triclinic, a = 12.870(2) Å, b = 13.638(2) Å, c = 9.514(2) Å, α = 109.59(1)°, β = 96.89(2)°, γ = 63.57(1)°, U = 1408.0(4) Å^3, T = 296.2 K, space group $P\bar{1}$ (no.2), Z = 2, μ(Mo-K_α) = 0.71 cm^{-1}, 6738 reflections measured, 6467 unique (R_{int} = 0.029) which were used in all calculations. The final R indices [$I > 2\sigma(I)$], R_1 = 0.0611, $wR(F^2)$ = 0.1447.

Inclusion Compound 1c·Chloroform: Crystals of **1c**·chloroform were recrystallized from chloroform as air-stable, greenish-yellow prisms. The one selected had approximate dimensions of 0.50 × 0.40 × 0.65 mm. The transmission factors ranged from 0.98 to 1.00. The crystal structure was solved by direct methods by using SIR 92.[12] The structures were expanded by using Fourier techniques.[13] The non-hydrogen atoms were refined anisotropically. Some hydrogen atoms were refined isotropically, the rest were fixed geometrically and not refined. Crystal data: $C_{31}H_{32}NO_3Cl_3$, M = 572.96, triclinic, a = 11.463(2) Å, b = 13.591(3) Å, c = 10.556(2) Å, α = 97.01(2)°, β = 113.75(1)°, γ = 98.15(2)°, U = 1460.6(6) Å^3, T = 296.2 K, space group $P\bar{1}$ (no.2), Z = 2, μ(Mo-K_α) = 3.5 cm^{-1}, 5426 reflections measured, 5147 unique (R_{int} = 0.029) which were used in all calculations. The final R indices [$I > 2\sigma(I)$], R_1 = 0.0782, $wR(F^2)$ = 0.1883.

Acknowledgments

This work was partially supported by a Grant-in-Aid for Science and Research from the Ministry of Education, Science, Sport and Culture of Japan (Grant 18350100) and by a Special Research Grant for Green Science from Kochi University.

[1] a) B. Valeur, *Molecular Fluorescence*, VCH, Weinheim, **2002**; b) K. Köller, *Appl. Fluoresc. Technol.* **1989**, *1*, 1.

[2] a) A. W. Gzarnik (Ed.), *Fluorescent Chemosensors for Ion and Molecule Recoginition*, ACS Symposium Series No. 538, American Chemical Society, Washington, DC, **1992**; b) A. W. Czarnik, *Acc. Chem. Res.* **1994**, *27*, 302; c) A. P. de Silva, H. Q. N. Gunaratne, T. Gunnlaugsson, A. J. M. Huxley, C. P. McCoy, J. T. Rademacher, T. E. Rice, *Chem. Rev.* **1997**, *97*, 1515–1566; d) G. Klein, J.-S. Reymond, *Angew. Chem. Int. Ed.* **2001**, *40*, 1711–1773; e) G. Klein, D. Kaufmann, S. Schurch, J.-S. Reymond, *Chem. Commun.* **2001**, 561–562.

[3] a) E. Weber, K. Skobridis, I. Goldberg, *J. Chem. Soc., Chem. Commun.* **1989**, 1195–1197; b) T. H. Brehmer, P. P. Korkas, E. Weber, *Sens. Actuators, B* **1997**, *44*, 595–600; c) E. Weber, T. Hens, Q. Li, T. C. W. Mark, *Eur. J. Org. Chem.* **1999**, 1115–1125; d) Z. Fei, N. Kocher, C. J. Mohrschladt, H. Ihmels, D. Stalke, *Angew. Chem. Int. Ed.* **2003**, *42*, 783–787; e) J. L. Scott, T. Yamada, K. Tanaka, *New J. Chem.* **2004**, *28*, 447–450.

[4] a) K. Yoshida, H. Miyazaki, Y. Miura, Y. Ooyama, S. Watanabe, *Chem. Lett.* **1999**, 837–838; b) K. Yoshida, Y. Ooyama, S. Tanikawa, S. Watanabe, *Chem. Lett.* **2000**, 714–715; c) K. Yoshida, Y. Ooyama, S. Tanikawa, S. Watanabe, *J. Chem. Soc. Perkin Trans. 2* **2002**, 708–714; d) Y. Ooyama, T. Mamura, K. Yoshida, *Eur. J. Org. Chem.* **2007**, *30*, 5010–5019.

[5] a) Y. Ooyama, T. Nakamura, K. Yoshida, *New J. Chem.* **2005**, *29*, 447–456; b) Y. Ooyama, K. Yoshida, *New J. Chem.* **2005**, *29*, 1204–1212.

[6] K. Yoshida, K. Uwada, H. Kumaoka, L. Bu, S. Watanabe, *Chem. Lett.* **2001**, 808–809.

[7] Y. Ooyama, T. Okamoto, T. Yamaguchi, T. Suzuki, A. Hayashi, K. Yoshida, *Chem. Eur. J.* **2006**, *12*, 7827–7838.

[8] a) E. Horiguchi, S. Matsumoto, K. Funabiki, M. Matsui, *Bull. Chem. Soc. Jpn.* **2005**, *78*, 1167–1173.

[9] A. Ortiz, W. H. Flora, G. D. D'Ambruoso, N. R. Armstrong, D. V. McGrath, *Chem. Commun.* **2005**, 444–446.

[10] a) Y. Ooyama, Y. Harima, *Chem. Lett.* **2006**, 902; b) Y. Ooyama, Y. Kagawa, Y. Harima, *Eur. J. Org. Chem.* **2007**, 3613.

[11] *teXsan*: Crystal Structure Analysis Package, Molecular Structure Corporation **1985** and **1992**.

[12] A. Altomare, M. C. Burla, M. Camalli, M. Cascarano, C. Giacovazzo, A. Guagliardi, G. Polidori, *J. Appl. Crystallogr.* **1994**, *27*, 435.

[13] P. T. Beurskens, G. Admiraal, G. Beurskens, W. P. Bosman, R. de Gelder, R. Israel, J. M. M. Smits, *The DIRIF94 Program System*, Technical Report of the Crystallography Laboratory, University of Nijmegen, The Netherlands, **1994**.

Received: January 15, 2008
Published Online: April 1, 2008

